Molecular Neurobiology (2019) 56:267–277
https://doi.org/10.1007/s12035-018-0994-z

Ursodeoxycholic Acid Inhibits Inflammatory Responses and Promotes Functional Recovery After Spinal Cord Injury in Rats

Wan-Kyu Ko[1] · Seong Jun Kim[1] · Min-Jae Jo[1] · Hyemin Choi[1] · Donghyun Lee[2] · Il Keun Kwon[3] · Soo-Hong Lee[4] · In-Bo Han[1] · Seil Sohn[1]

Received: 1 December 2017 / Accepted: 7 March 2018 / Published online: 20 March 2018

Abstract

The aim of this study was to investigate the anti-inflammatory effects by ursodeoxycholic acid (UDCA) in rats with a spinal cord injury (SCI). A moderate mechanical compression injury was imposed on adult Sprague-Dawley (SD) rats. The post-injury locomotor functions were assessed using the Basso, Beattie, and Bresnahan (BBB) locomotor scale and the tissue volume of the injured region was analyzed using hematoxylin and eosin staining. The pro-inflammatory factors were evaluated by immunofluorescence (IF) staining, a quantitative real-time polymerase chain reaction (qRT-PCR), and enzyme-linked immunosorbent assay (ELISA). The phosphorylation of the extracellular signal-regulated kinase (ERK), c-Jun N-terminal kinase (JNK), and p38 in mitogen-activated protein kinase (MAPK) signaling pathways related to inflammatory responses were measured by Western blot assays. UDCA improved the BBB scores and promoted the recovery of the spinal cord lesions. UDCA inhibited the expression of glial fibrillary acidic protein (GFAP), tumor necrosis factor-α (TNF-α), ionized calcium-binding adapter molecule 1 (iba1), and inducible nitric oxide synthase (iNOS). UDCA decreased the pro-inflammatory cytokines of TNF-α, interleukin 1-β (IL-1β), and interleukin 6 (IL-6) in the mRNA and protein levels. UDCA increased the anti-inflammatory cytokine interleukin 10 (IL-10) in the mRNA and protein levels. UDCA suppressed the phosphorylation of ERK, JNK, and the p38 signals. UDCA reduces pro-inflammatory responses and promotes functional recovery in SCI in rats. These results suggest that UDCA is a potential therapeutic drug for SCI.

Keywords Ursodeoxycholic acid · Spinal cord injury · BBB score · MAPK signaling · TNF-α · Anti-inflammation

Introduction

Spinal cord injuries (SCI) cause marked neuropathology and are associated with limited functional recovery [1]. In addition, the injured spinal cord physiologically induces secondary damage such as apoptotic cell death of affected neurons and glia [2, 3] as well as the production of inflammatory mediators [4]. With regard to these types of secondary damage, numerous researchers have attempted to suppress inflammatory responses after SCI [5–7].

While the extent of the primary injury is determined by the initial trauma, which is typically beyond the control of caregivers, the severity of secondary pro-inflammatory injuries can potentially be modulated using pharmacological agents such as methylprednisolone (MP). Although MP has been used as an anti-inflammatory drug [8], it causes adverse side effects, including wound infections, pneumonia, and acute corticosteroid myopathy [9, 10].

Ursodeoxycholic acid (UDCA), a hydrophilic bile acid, has been used in Chinese medicine for more than 3000 years [11]. UDCA was originally approved by the US Food and Drug Administration (FDA) for the treatment of several cholestatic liver disorders [12]. Specifically, UDCA is widely used for the treatment of hepatic diseases, such as gallstones, chronic hepatitis, and primary biliary cirrhosis [13–15]. In other words,

Electronic supplementary material The online version of this article (https://doi.org/10.1007/s12035-018-0994-z) contains supplementary material, which is available to authorized users.

✉ In-Bo Han
hanib@cha.ac.kr

✉ Seil Sohn
sisohn@cha.ac.kr

[1] Department of Neurosurgery, CHA Bundang Medical Center, CHA University, 59, Yatap-ro, Bundang-gu, Seongnam-si, Gyeonggi-do 13496, Republic of Korea

[2] Department of Dentistry, Graduate School, Kyung Hee University, Dongdaemun-gu, Seoul 02447, Republic of Korea

[3] Department of Dental Materials, School of Dentistry, Kyung Hee University, Dongdaemun-gu, Seoul 02447, Republic of Korea

[4] Department of Biomedical Science, CHA University, Seongnam-si, Gyeonggi-do 13488, Republic of Korea

the effects of UDCA are mainly linked to efforts to remedy damage to hepatocytes.

In a recent study by the authors, we evaluated the anti-inflammatory effect of UDCA using LPS-stimulated RAW 264.7 macrophages in vitro [16]. The inflammatory response in an injured human spinal cord is largely similar to that observed in rodents [17, 18]. Thus, we aimed to evaluate the effects of UDCA as an anti-inflammatory drug in SCI rats.

Materials and Methods

Subjects

Eighty-one adult female Sprague-Dawley (SD) rats (200–220 g) as used in this study were purchased from Orient Bio Inc. (Seongnam, Korea), housed in a facility at 55–65% humidity and a controlled temperature of 24 ± 3 °C with a light/dark cycle of 12 h, and given free access to water and food. All surgical interventions and postoperative animal care procedures were performed in accordance with the Guidelines and Policies for Rodent Survival Surgery provided by the Institutional Animal Care Committee (IACUC) of CHA University (IACUC160074).

Modeling of Animals

The animals were anesthetized with a Zoletil® (50 mg/kg, Virbac Laboratories, France)/Rompun® (10 mg/kg, Bayer, Korea) solution administered intraperitoneally. Complete anesthesia was assessed using the hindlimb withdrawal reflex in response to a noxious foot pinch. After skin preparation and precise positioning of the anesthetized rats, the ninth thoracic spinal cord segment (T9) was exposed by laminectomy. The vertebral column was supported and stabilized by Allis clamps at the T7 and T11 spinous processes using a method described previously [19]. A metal impounder (35 g) was then gently applied onto the T9 dura for 5 minutes, resulting in moderate standing weight compression. After the compression injury, the surgical site was closed by suturing the muscle and fascia and suturing the skin, followed by an external povidone-iodine application. All surgical procedures were performed by the same person (S Sohn), and the animals for the sham groups underwent a T9 laminectomy without weight compression injury.

Experimental Groups

We randomly divided all rats into three groups: the laminectomy-only group ($n = 27$, sham group), the normal saline (NS) injection after injury group ($n = 27$, injury + NS group), and the UDCA injection after injury group ($n = 27$, injury + UDCA group). The predetermined experimental day was 1, 3, or 7 days after the injury. Nine rats per group were sacrificed and analyzed each day for hematoxylin and eosin (H&E) and immunofluorescence (IF) staining ($n = 3$), quantitative real-time polymerase chain reactions (qRT-PCR, $n = 3$), enzyme-linked immunosorbent assay (ELISA), and Western blot assays ($n = 3$). The bladders of the injured animals were manually emptied twice daily until normal function returned.

Administrations of UDCA

Sodium ursodeoxycholate hydrate was obtained from TCI (Tokyo Chemical Industry Co., Ltd., Japan) and solubilized in sterilized NS for the injections. A total of 25 mg/kg/day of UDCA (in a volume of 250 μL) or 250 μL of NS was injected intraperitoneally immediately after SCI in the injury + UDCA and injury + NS groups. The solutions were then also given once a day for 3 or 7 days at the indicated time points, as described in Fig. 1. The UDCA solutions were prepared immediately before the experiments. Three rats per group on predetermined days were anesthetized and sacrificed by intra-cardiac perfusion with saline for H&E and IF staining. The other six rats per group were euthanized by CO_2 asphyxiation and the spinal cords were removed for qRT-PCR and Western blot assays.

Behavioral Tests

Briefly, two trained investigators who were blind to the experimental conditions performed the behavioral analyses. To test the hindlimb locomotor function, open-field locomotion was evaluated using the Basso, Beattie, and Bresnahan (BBB) locomotion scale, as previously described [20]. BBB is a 22-point scale (with scores of 0–21) that systematically and logically follows the recovery of hindlimb function from a score of 0, indicative of no observed hindlimb movements, to a score of 21, representative of a normal ambulating rodent. Five rats per group were measured daily for 7 days.

Tissue Preparation for Histological Analysis

On predetermined days, three rats per group were perfused transcardially with PBS followed by 4% paraformaldehyde in PBS via a method previously described [21]. The length of the spinal cord was 10 mm from the rostral to caudal sections, including the epicenter lesion. The spinal cords were post-fixed overnight in the same 4% paraformaldehyde, embedded in paraffin, and dewaxed for a histological analysis. Serial longitudinal sections through the dorsoventral axis of the spinal cord (5 μm thick) were collected at lengths of every 100 μm (20th) and 105 μm (21st) per rat. The 20th section for each rat was used for H&E staining and for quantification of

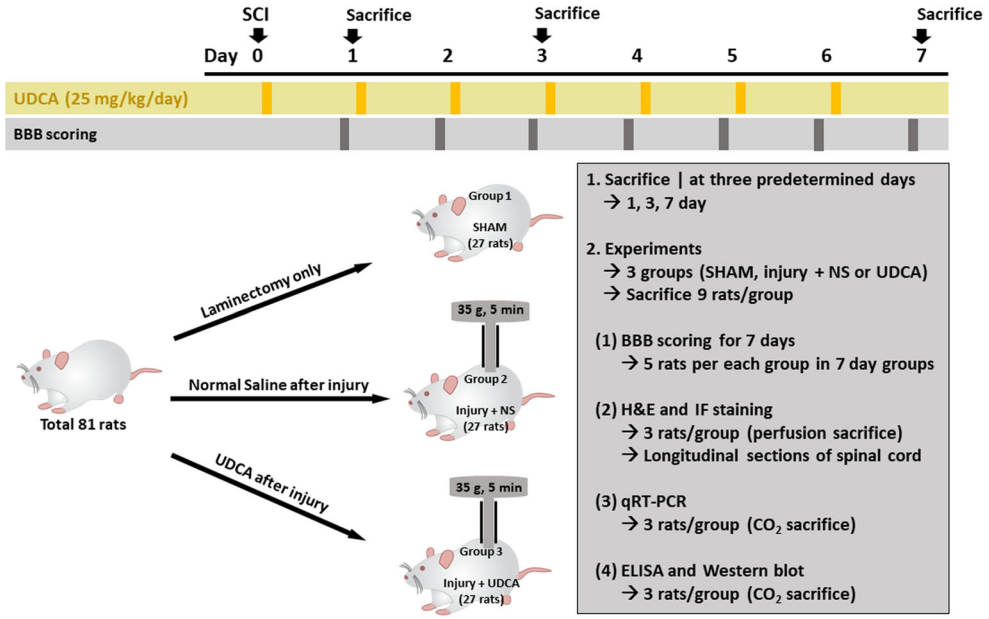

Fig. 1 Scheme of the experimental design. For rats in the injury groups, a metal impounder (35 g) was gently applied on the T9 dura for 5 min, resulting in a moderate spinal cord injury (SCI). The vertebral column was supported and stabilized by Allis clamps at the T7 and T11 spinous processes. Normal saline (NS) alone (250 μL) or NS containing UDCA (25 mg/kg density in 250 μL NS) was administered intraperitoneally immediately after the injury and once daily for 1, 3, or 7 days. The rats were randomly divided into three groups: the laminectomy-only group ($n = 27$, sham group), the NS injection after injury group ($n = 27$, injury + NS group), and the UDCA injection after injury group ($n = 27$, injury + UDCA group). Nine rats on each day were sacrificed and analyzed by hematoxylin and eosin (H&E) and immunofluorescence (IF) staining ($n = 3$), quantitative real-time polymerase chain reaction (qRT-PCR, $n = 3$), ELISA, or Western blot experiments ($n = 3$)

the tissue volume. The 21st section for each rat was used for IF staining and for quantification of the intensity levels. At each section, the most severely injured site of the spinal cord was selected as the region of interest (ROI, 500 × 300 μm). The morphological changes of the H&E-stained tissues and IF images of glial fibrillary acidic protein (GFAP), tumor necrosis factor-α (TNF-α), ionized calcium-binding adapter molecule 1 (iba1), and inducible nitric oxide synthase (iNOS) were observed at × 40 (scale bar, 500 μm) and × 400 (scale bar, 50 μm) magnification using a light microscope and an inverted fluorescence microscope, respectively (Olympus IX71, Japan).

Quantification of Tissue Volume

The serial longitudinal sections through the dorsoventral axis of the spinal cord (5 μm thick) were collected at lengths of every 100 μm (20th), and the 20th section was stained with an H&E solution (BBC Biochemical, Mount Vernon, USA). On the 20th section for three rats per group/predetermined day, we randomly designated two rectangular areas (200 × 125 μm, for a total of six images/group/1, 3, or 7 days) in the ROI (500 × 300 μm) for quantification of the tissue volume. The randomly and blindly selected rectangular area of 200 × 125 μm in the ROI was represented 100% and the filled tissue volume was calculated and quantified using the ImageJ software (http://rsb.info.nih.gov/ij/index.html, ImageJ; National Institutes of Health (NIH), Bethesda, MD, USA).

Immunofluorescence Staining of GFAP, TNF-α, iba1, and iNOS

Serial longitudinal sections through the dorsoventral axis of the spinal cord (5 μm thick) were collected every 105 μm (21st) and the 21st section was double-stained against GFAP and TNF-α. Every 110 μm (22nd), the 22nd section was double-stained against iba1 and iNOS. The 21st sections were treated with a blocking solution to prevent a nonspecific binding reaction for 1 h and then stained by incubation overnight at 4 °C with the following primary antibodies in PBS: monoclonal mouse anti-mouse GFAP (1:200; Sigma, St. Louis, USA) and polyclonal anti-rabbit TNF-α (1:200; Abcam, Cambridge, UK). The 22nd sections were treated with polyclonal anti-goat iba1 (1:200; Abcam) and polyclonal anti-rabbit iNOS (1:200; Abcam). The 21st sections were then incubated with fluorescent secondary donkey anti-mouse Alexa 568 and donkey anti-rabbit Alexa 488 in a blocking solution (1:400; Invitrogen Life Sciences, Carlsbad, CA, USA) for 1 h at room temperature. The 22nd sections were incubated with fluorescent secondary donkey anti-goat 594 and donkey anti-rabbit Alexa 488. At the end of the process, nuclei were stained with

Table 1 Nucleotide sequences of primers used in real-time qRT-PCR

Gene	(5′–3′)	Reverse (5′–3′)
TNF-α	TACTCCCAGGTTCTCTTCAA	CCAGGCTGACTTTCTCCTGG
IL-1β	TGCTGATGTACCAGTTGGGG	CTCCATGAGCTTTGTACAAG
IL-6	CGAGCCCACCAGGAACGAAAGTC	CTGGCTGGAAGTCTCTTGCGGAG
IL-10	TGGACAACATACTGCTGACAG	GGTAAAACTTGATCATTTCTGACAAG
GAPDH	ATGATTCTACCCACGGCAAG	CTGGAAGATGGTGATGGGTT

DAPI and sections were washed with PBS and mounted with a specific medium (Dako Cytomation, Milan, Italy).

Quantification of GFAP, TNF-α, iba1, and iNOS

Serial longitudinal sections through the dorsoventral axis of the spinal cord (5 μm thick) were collected every 105 and 110 μm (21st and 22nd) from three rats per group/predetermined day. We randomly designated two rectangular areas (200 × 125 μm, for a total of six images/group/1, 3, or 7 days) in the ROI (500 × 300 μm) for the quantification of the GFAP, TNF-α, iba1, and iNOS intensities in × 400 magnifications. The area of the captured images under × 400 magnification (200 × 125 μm) was 1,392,640 (1360 × 1024) pixels. The stained immunofluorescence pixels per image were calculated and quantified using an intensity measurement method available in the ImageJ software package (NIH) [22].

RNA Extraction and qRT-PCR

Segments of the spinal cord (10 mm) including the lesion epicenter were collected at 1, 3, and 7 days after SCI. The segments were homogenized using a T 25 digital homogenizer (IKA, Seoul, Korea) in TRIzol reagent (Invitrogen, Life Sciences, Carlsbad, CA, USA) according to the manufacturer's instructions for RNA extraction. Complementary DNA (cDNA) was synthesized from 1 μg of the total RNA using a synthesis kit (Takara Bio, Shiga, Japan) and qRT-PCR was conducted using an ABI StepOne Real-time PCR System (Applied Biosystems, Warrington, UK). The PCR protocol consisted of 40 cycles of denaturation at 95 °C for 15 s, followed by 60 °C for 30 s to allow for extension and amplification of the target sequence. The relative expression levels of TNF-α, IL-1β, IL-6, and IL-10 were normalized to that of glyceraldehyde 3-phosphate dehydrogenase (GAPDH) using

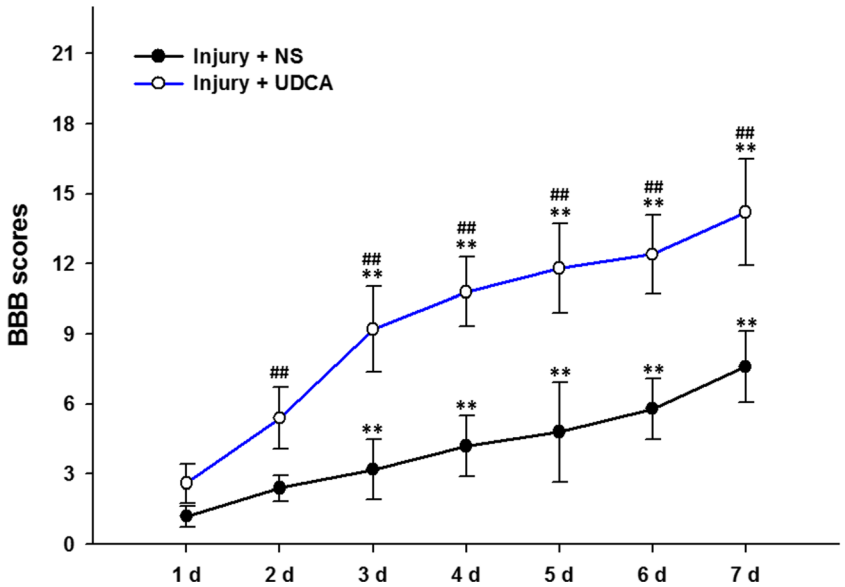

Fig. 2 Comparison of Basso, Beattie, and Bresnahan (BBB) locomotor scores in the injury + NS and injury + UDCA group. The BBB scores in the injury + NS and injury + UDCA groups were evaluated for 7 days after injury. Five rats/group of the 7-day experimental group were measured for 7 days. The injury + UDCA group received intraperitoneal injections of 25 mg/kg of UDCA (solubilized in 250 μL NS) immediately after injury and daily intervals thereafter for 7 days. The injury + NS group received intraperitoneal injections of the same volume of NS at daily intervals for 7 days. The results are the mean ± SD; significant differences as compared to the day 1 scores within each group were demonstrated daily (*$p < 0.05$, **$p < 0.01$). A significant difference between the injury + UDCA group and the injury + NS group was also demonstrated ($^{\#\#}p < 0.01$)

the $2^{-\Delta\Delta CT}$ method [23]. The primers were obtained from Bioneer (Daejeon, Korea). The primer sequences used in this study are shown in Table 1. These experiments were repeated three times.

Enzyme-Linked Immunosorbent Assay (ELISA) and Western Blotting

Segments of the spinal cord (10 mm) including the lesion epicenter at the middle were collected at 1, 3 and 7 days after SCI. The segments were collected and washed with PBS, placed at 4 °C, and homogenized using a T 25 digital homogenizer (IKA) in lysis buffer (1× RIPA lysis buffer), after which they were centrifuged at 14,000 rpm at a temperature of 4 °C for 15 min. Protein concentrations in tissue lysates were measured with the aid of a BCA protein assay kit (Thermo Scientific, Rockford, IL). The ELISA kits for TNF-α, IL-1β, IL-6, and IL-10 were from Koma Biotech (Seoul, Korea). The content of each segment was obtained according to the standard curve at 450 nm. For the Western blot assay, equal amounts of protein (40 μg) were subjected to SDS-PAGE gel electrophoresis and transferred to nitrocellulose membranes. The membranes were incubated with 5% skim milk for 1 h to block the nonspecific binding and then probed with the primary antibodies of the phosphorylated forms of extracellular signal-regulated kinase (p-ERK, 1:1000), c-Jun N-terminal kinase (p-JNK, 1:1000), and p38 (p-p38, 1:1000). Subsequently, equal membranes were stripped and reprobed with the total forms of ERK (t-ERK, 1:1000), JNK (t-JNK, 1:1000), and p38 (t-p38, 1:1000). All of the primary antibodies were purchased from Cell Signaling Technology (Danvers, MA, USA) except for β-actin (1:2000, Abcam, Cambridge, UK). As an internal control, β-actin was also probed into the membranes. All primary markers were followed by incubation with secondary antibodies (1:5000, Santa Cruz Biotechnology, Dallas, TX). The visualized signal bands were detected using an ECL solution (Amersham, Buckinghamshire, UK) through the ChemiDoc XRS System (Bio-Rad, Hercules, USA). The phosphorylated form/total form (*p*/*t* form) volumes for the predetermined days were calculated and quantified using ImageJ software (NIH). The *p*/*t* form volume of the 1-day sham group was set at onefold and the ratio of the normalized fold change was relatively calculated and quantified for 7 days. These experiments were repeated three times.

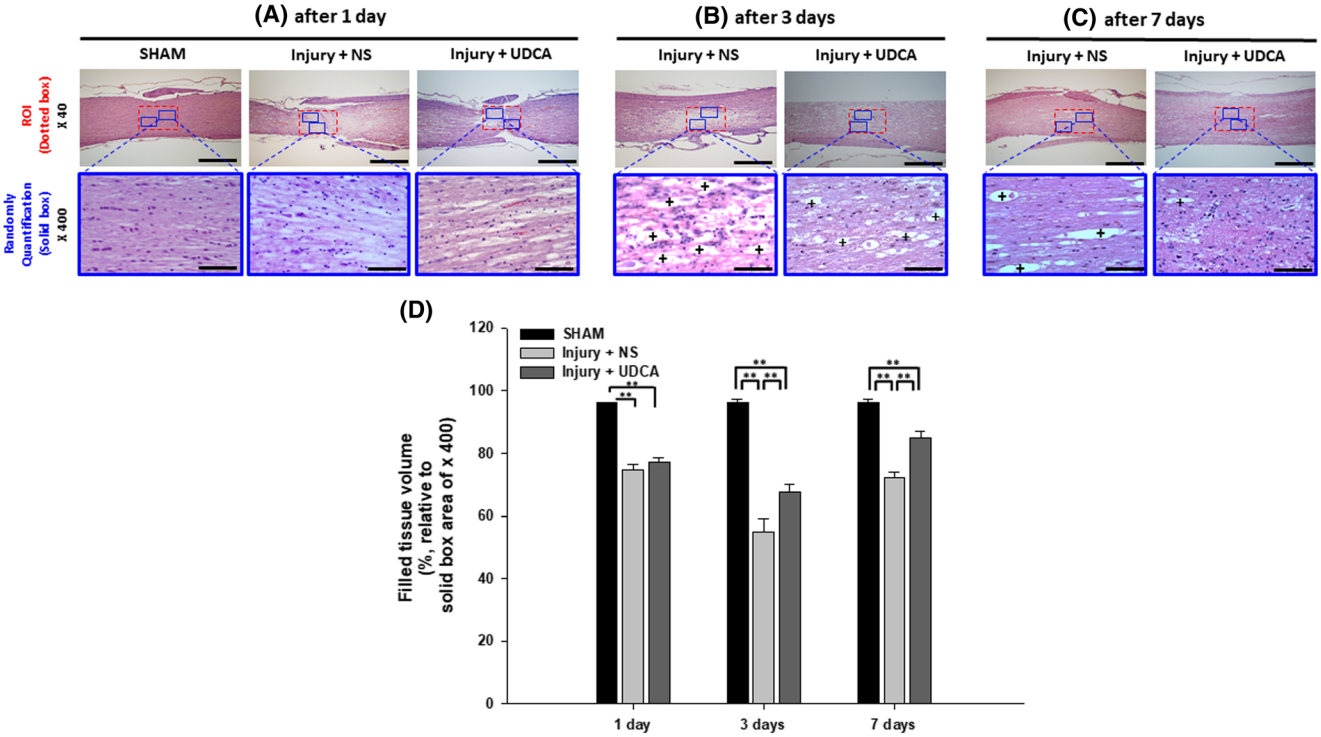

Fig. 3 H&E staining and quantification of the cavity volume in injured spinal cords. H&E staining outcomes in the lesions of the ROIs were observed under × 40 (scale bar, 500 μm) and × 400 (scale bar, 50 μm) magnification. **a** On day 1 after SCI, the expressions of the filled tissue volume in sham, injury + NS, and injury + UDCA groups are shown. **b** On day 3 after SCI, the expressions of the filled tissue volume in the injury + NS and injury + UDCA groups are shown. **c** On day 7 after SCI, the expressions of the filled tissue volume in injury + NS and injury + UDCA groups are shown. **d** Quantitative analysis of the filled tissue volume. Results are the mean ± SEM: $*p < 0.05$ and $**p < 0.01$, significant differences among three groups were demonstrated

Statistical Analyses

All values are presented as the mean ± standard error of the mean (SEM). Behavioral scores were analyzed by Student's *t* tests. Multiple comparisons among groups were performed with a one-way analysis of variance (ANOVA), and Tukey's multiple-comparison test was used as a post hoc analysis method. Differences with *p* values for which $*p < 0.05$ and $**p < 0.01$ were considered statistically significant.

Results

UDCA Improved Functional Recovery after SCI

To assess functional recovery by UDCA, BBB scores were measured during 1 week after injury. The BBB scores for the hindlimb motor function in the injury + NS group improved from 1.20 ± 0.45 on day 1 to 7.60 ± 1.52 on day 7 (Fig. 2). Figure 2 shows that the scores in the injury + UDCA group demonstrated a significant improvement from 2.80 ± 0.84 on day 1 to 14.20 ± 2.28 on day 7 after SCI ($**p < 0.01$). Figure 2 also indicates that the BBB scores in the injury + UDCA group significantly increased compared to those in the injury + NS group on each day ($^{\#\#}p < 0.01$). The scores in the sham group were constant at 21 for 7 days (data not shown).

UDCA Promoted the Recovery of Tissue Cavities after SCI

We performed H&E staining whether UDCA promoted the recovery of injured tissue. On day 1 after SCI, the spinal cord tissues showed apparent areas of structural damage in both the injury + NS and injury + UDCA groups. Distinct recovery was not shown in the injury + UDCA group on day 1 (Fig. 3a). On day 3 after SCI, however, the lesion of the tissue showed obvious cavities (as indicated by "+") in the injury + NS group, and the volume of lesion in the injury + UDCA group was reduced (Fig. 3b). On day 7 after SCI, the cavities of the lesion in the injury + UDCA group were also reduced as compared to that observed in the injury + NS group. Figure 3d demonstrates that the tissue volume of the randomly

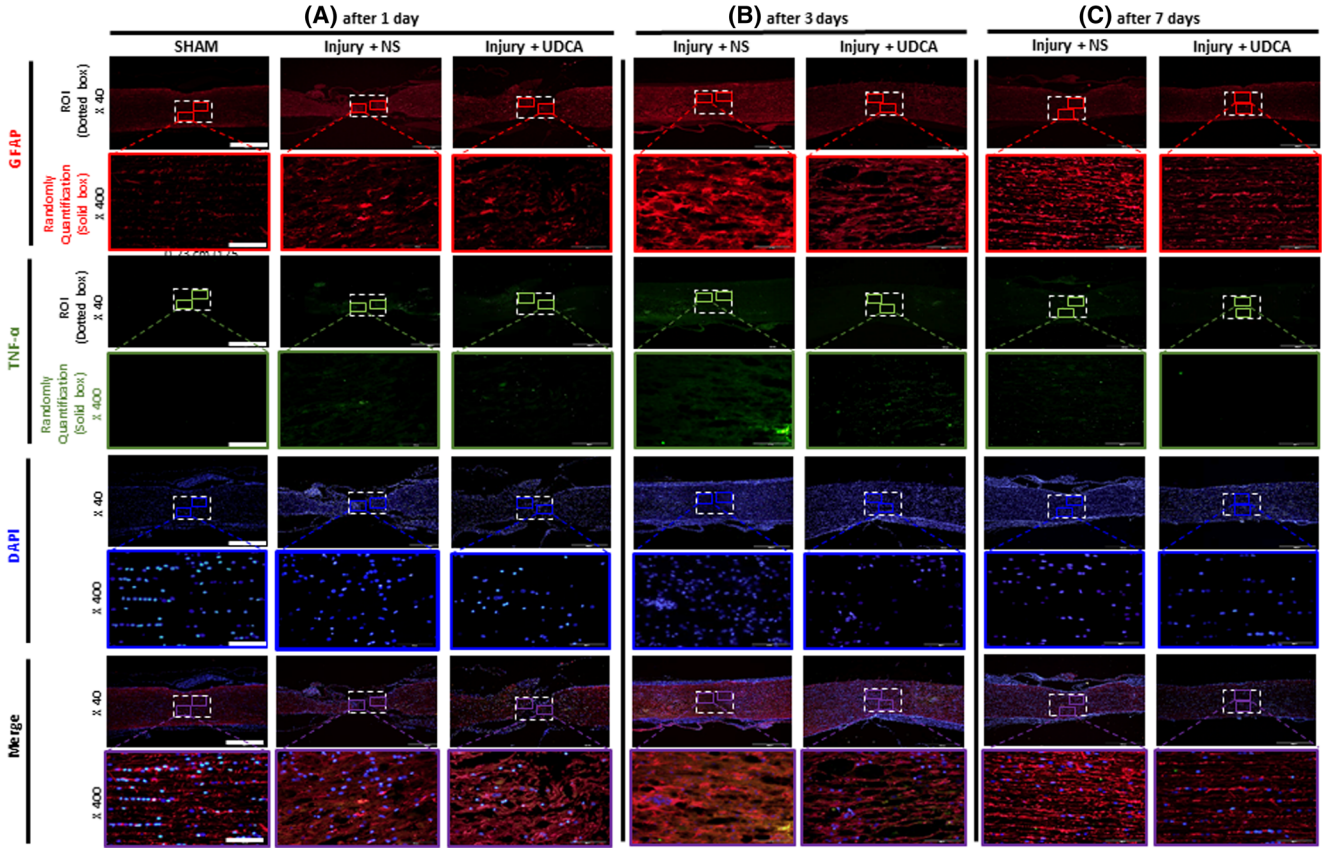

Fig. 4 Immunofluorescence staining of GFAP and TNF-α. Immunofluorescence staining outcomes in the lesions of the ROIs were observed under × 40 (scale bar = 500 μm) and × 400 (scale bar = 50 μm) magnification. **a** On day 1 after SCI, the expressions of GFAP and TNF-α in the sham, injury + NS, and injury + UDCA groups are shown. **b** On day 3 after SCI, the expressions of GFAP and TNF-α in the injury + NS and injury + UDCA groups are shown. **c** On day 7 after SCI, the expressions of GFAP and TNF-α in the injury + NS and injury + UDCA groups are shown

designated ROI was significantly increased in the injury + UDCA group (67.70% ± 2.30) compared to that of the injury + NS group (54.93% ± 4.22) on day 3 (**$p < 0.01$). In addition, the tissue volume was significantly increased in the injury + UDCA group (84.87% ± 2.07) compared to that of the injury + NS group (72.38% ± 1.77) on day 7 (**$p < 0.01$).

UDCA Inhibited the Expression of GFAP, TNF-α, iba1, and iNOS after SCI

In order to evaluate whether UDCA inhibited the inflammatory responses in the lesion of spinal cord, we examined the immunoreactivities for GFAP, TNF-α, iba1, and iNOS. GFAP and TNF-α fluorescence were slightly expressed in the sham groups for 7 days (Fig. 4a–c, sham images at 3 and 7 days not shown). The fluorescence of GFAP and TNF-α in the injury groups for 7 days is also presented in Fig. 4a–c. On day 3, the GFAP intensity in the injury + UDCA group (494,181 ± 18,627) was significantly decreased as compared to that in the injury + NS group (773,477 ± 41,309, **$p < 0.01$, Fig. S1a). TNF-α intensity in the injury + UDCA group (217,451 ± 13,285) was also significantly decreased as compared to that in the injury + NS group (616,215 ± 34,845) after 3 days (**$p < 0.01$, Fig. S1b). On day 7, the GFAP intensity in the injury + UDCA group (314,541 ± 17,869) was significantly decreased as compared to that in the injury + NS group (565,384 ± 32,084, **$p < 0.01$, Fig. S1a). The TNF-α intensity in the injury + UDCA group (74,228 ± 4519) was also significantly decreased as compared to that in the injury + NS group on day 7 (155,997 ± 9659, **$p < 0.01$, Fig. S1b). The fluorescence of iba1 and iNOS in the injury groups for 7 days was presented in Fig. 5a–c. The increased iba1 and iNOS intensities by injury were decreased from 3 to 7 days by UDCA treatment (Fig. S2a, b).

UDCA Reduced the mRNA and Protein Expressions of Inflammatory Cytokines and Increased the mRNA and Protein Expression of an Anti-Inflammatory Cytokine, IL-10, After SCI

We conducted qRT-PCR and ELISA to determine whether UDCA inhibited the inflammatory responses in mRNA and

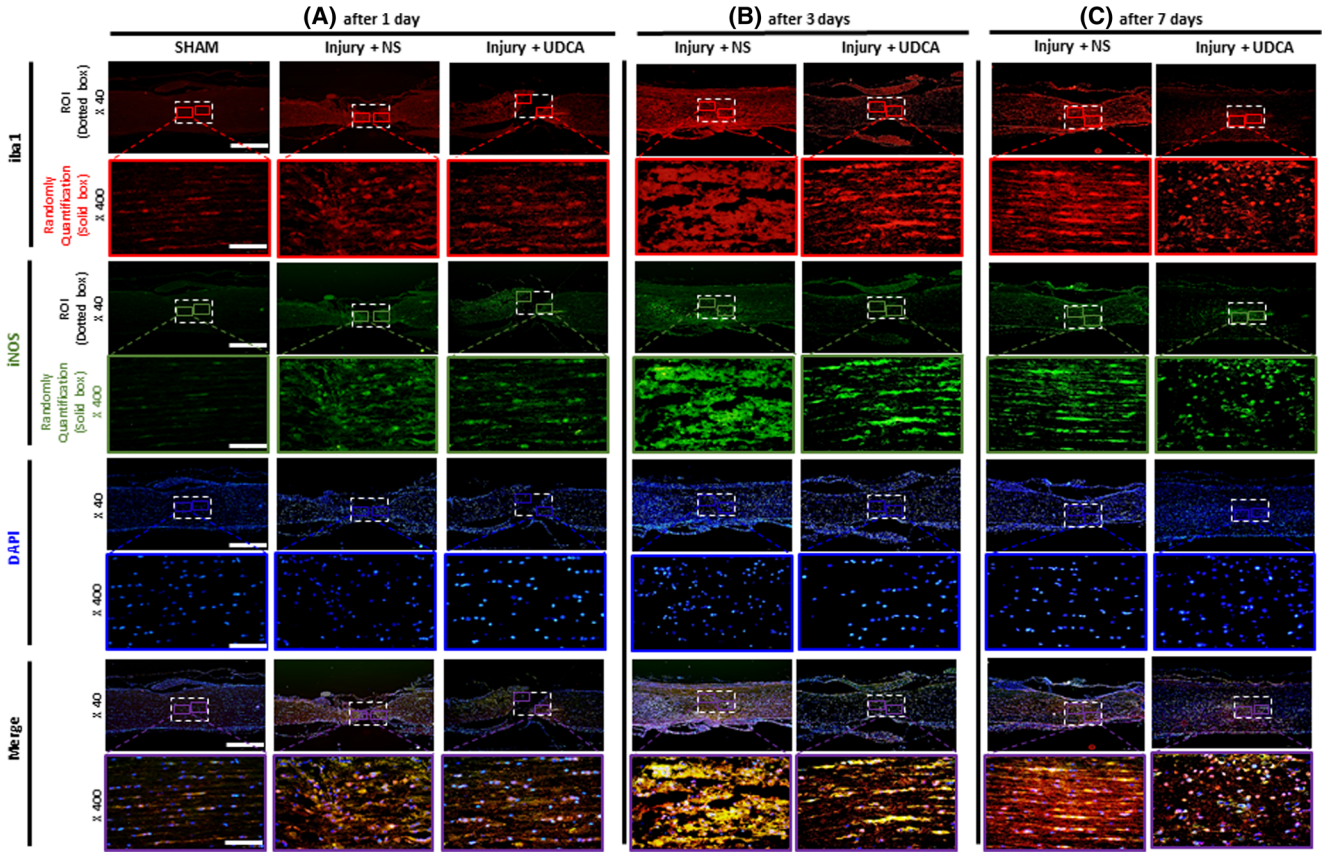

Fig. 5 Immunofluorescence staining of iba1 and iNOS. Immunofluorescence staining outcomes in the lesions of the ROIs were observed under × 40 (scale bar = 500 μm) and × 400 (scale bar = 50 μm) magnification. **a** On day 1 after SCI, the expressions of iba1 and iNOS in the sham, injury + NS, and injury + UDCA groups are shown. **b** On day 3 after SCI, the expressions of GFAP and TNF-α in the injury + NS and injury + UDCA groups are shown. **c** On day 7 after SCI, the expressions of iba1 and iNOS in the injury + NS and injury + UDCA groups are shown

protein levels. As shown in Fig. 6a–c, the inflammatory cytokines of TNF-α, IL-1β, and IL-6 were significantly inhibited by UDCA for 7 days (**$p < 0.05$). The TNF-α level in injury + NS groups (3.842 ± 0.154, 1.259 ± 0.104, and 0.689 ± 0.040 on days 1, 3, and 7, respectively) was increased after injury as compared to those in sham groups (1.000 ± 0.000, 0.423 ± 0.062, and 0.322 ± 0.026 on days 1, 3, and 7, respectively, Fig. 6a). However, UDCA significantly suppressed the expression of TNF-α mRNA (3.170 ± 0.166, 0.807 ± 0.043, and 0.499 ± 0.024 on days 1, 3, and 7, **$p < 0.01$, respectively) as compared to those in the injury + NS group (3.842 ± 0.154, 1.259 ± 0.104, and 0.689 ± 0.040 on days 1, 3, and 7, respectively, Fig. 6a). This suppression tendency by UDCA was also demonstrated in IL-1β and IL-6 mRNA (Fig. 6b, c). On the other hand, an anti-inflammatory cytokine, IL-10, was recorded at the maximum level at each time point in the injury + UDCA group (6.455 ± 0.423, 6.693 ± 0.408, and 6.969 ± 0.415 on days 1, 3, and 7, respectively, Fig. 6d). Similar inhibition tendency by UDCA was demonstrated in protein levels for 7 days (Fig. 7a–c). On the other hand, UDCA increased the anti-inflammatory cytokine such as IL-10 in protein levels (Fig. 7d).

Effect of UDCA on ERK, JNK, and p38 in Mitogen-Activated Protein Kinases After SCI

To determine whether UDCA inhibited the inflammatory signal pathways such as mitogen-activated protein kinases (MAPKs) including ERK and JNK and p38, we performed Western blot assays. The *p*/*t* volume of ERK was 6.95 ± 0.24 on day 3 in the injury + NS group, and it was significantly lower at 3.72 ± 0.18 in the injury + UDCA group (**$p < 0.01$,

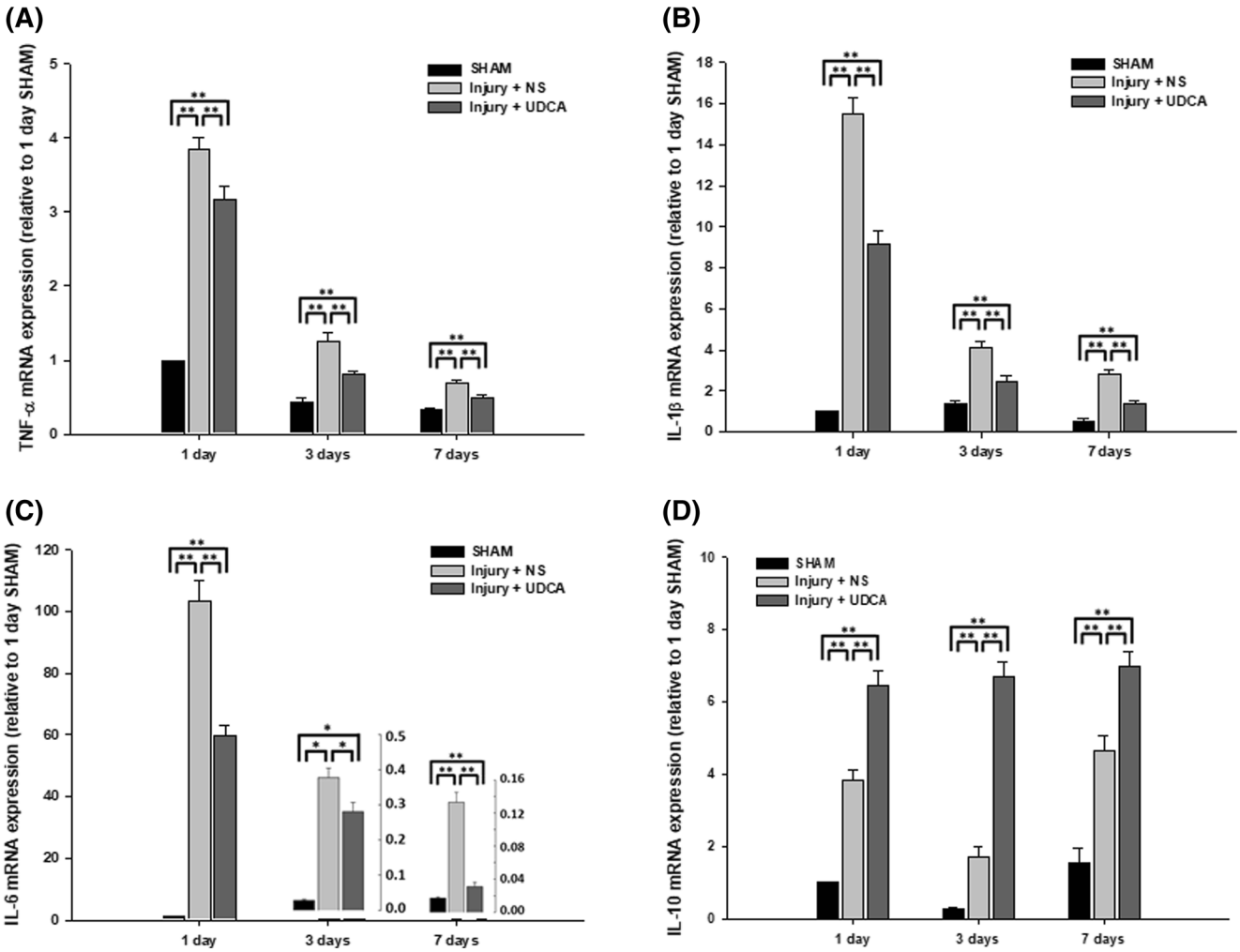

Fig. 6 The mRNA expression levels in the injured spinal cord segment treated with UDCA (25 mg/kg/day, solubilized in 250 μL NS) or NS alone (250 μL) for 1, 3, and 7 days. Segments of spinal cord (10 mm) including the lesion epicenter were collected on days 1, 3, or 7 after SCI. The relative expression levels of **a** TNF-α, **b** IL-1β, **c** IL-6, and **d** IL-10 were normalized to that of glyceraldehyde 3-phosphate dehydrogenase (GAPDH). The *p*/*t* form volume in the sham group of day 1 was set to onefold, and the ratio was relatively calculated and quantified. Results are the mean ± SEM: *$p < 0.05$ and **$p < 0.01$; significant differences among three groups were demonstrated

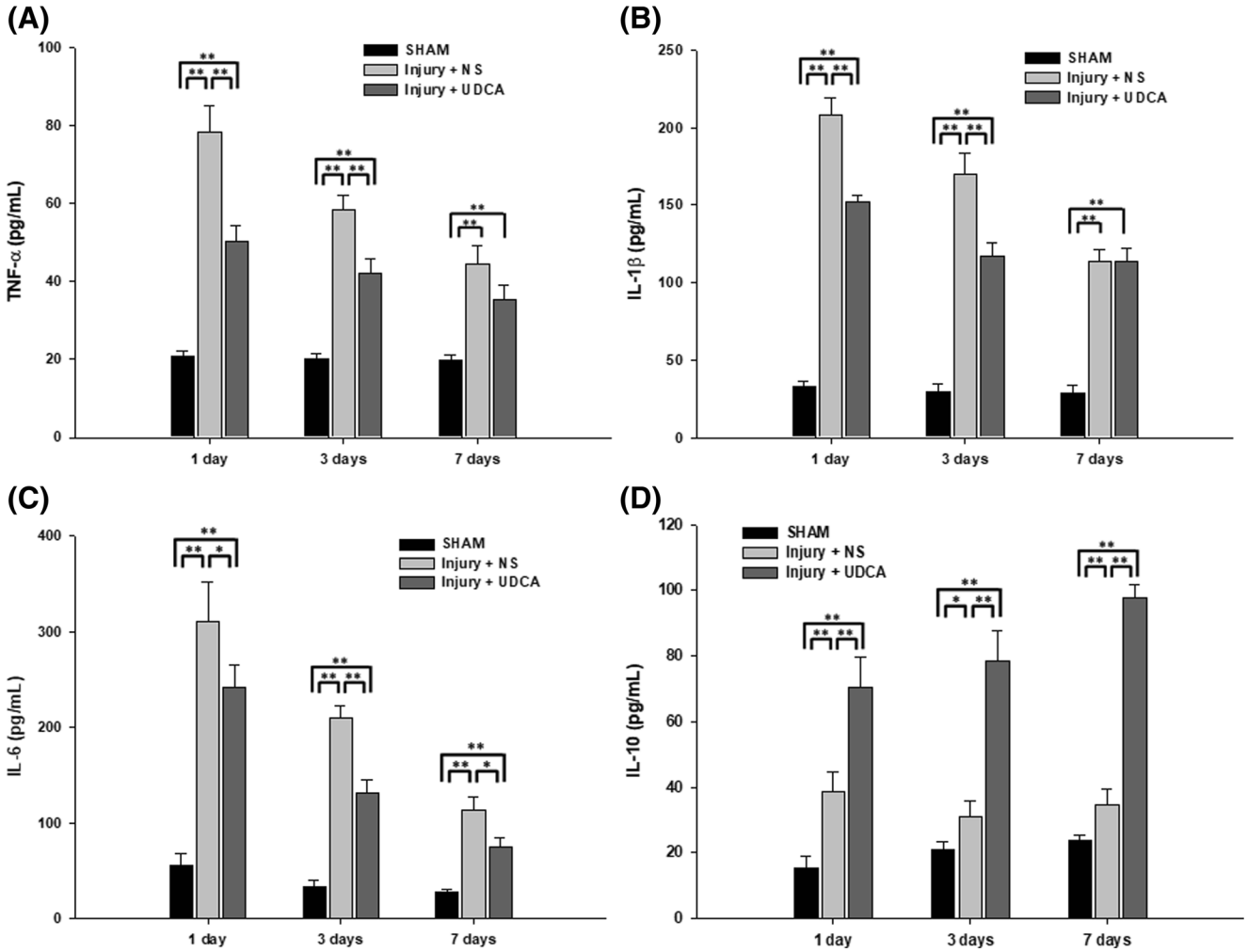

Fig. 7 The protein expression levels in the injured spinal cord segment treated with UDCA (25 mg/kg/day, solubilized in 250 μL NS) or NS alone (250 μL) for 1, 3, and 7 days. Segments of spinal cord (10 mm) including the lesion epicenter were collected on days 1, 3, or 7 after SCI. The relative expression levels of **a** TNF-α, **b** IL-1β, **c** IL-6, and **d** IL-10 were normalized to that of glyceraldehyde 3-phosphate dehydrogenase (GAPDH). The *p*/*t* form volume in the sham group of day 1 was set to onefold, and the ratio was relatively calculated and quantified. Results are the mean ± SEM: $*p < 0.05$ and $**p < 0.01$; significant differences among three groups were demonstrated

Fig. 8b). The *p*/*t* volumes of JNK and p38 in the injury + UDCA group were also significantly decreased (4.96 ± 0.27 and 1.17 ± 0.04, respectively) as compared to those in sham groups (1.24 ± 0.02 and 0.96 ± 0.02, respectively) on day 3 ($**p < 0.01$, Fig. 8d, f). The *p*/*t* volumes of the internal control, β-actin, were 0.97 ± 0.03 (sham group), 0.96 ± 0.01 (injury + NS group), and 0.99 ± 0.02 (injury + UDCA group) for 7 days (Fig. 8h).

Discussion

In this study, UDCA promoted functional recovery in SCI rats and it ameliorated histopathological damage to spinal cords. UDCA reduced the expression levels of the pro-inflammatory cytokines of TNF-α, IL-1β, and IL-6 after SCI. UDCA also increased the expression of an anti-inflammatory cytokine, IL-10, after SCI. In addition, the phosphorylation outcomes of ERK, JNK, and p38 in MAPK signal pathways were inhibited by UDCA in SCI rats.

Following SCI, resident microglia is activated and pro-inflammatory cytokines are upregulated, including TNF-α, IL-1β, IL-6, iba1, and iNOS [24, 25]. TNF-α is one of the major inflammatory cytokines and is an important component of the acute-phase injury reaction. Bethea et al. showed that the reduction of TNF-α promoted functional recovery following SCI [26]; their results were in accordance with the findings here (Fig. 2). The BBB scores in the injury + UDCA group steadily increased from day 2 after SCI (Fig. 2), and the expression level of TNF-α was significantly suppressed in the injury + UDCA group as compared to that in the injury + NS group on days 1, 3, and 7 (Figs. S1b, 6a, and 7a). The reduction of TNF-α by the UDCA treatment may affect the functional recovery outcomes in our study.

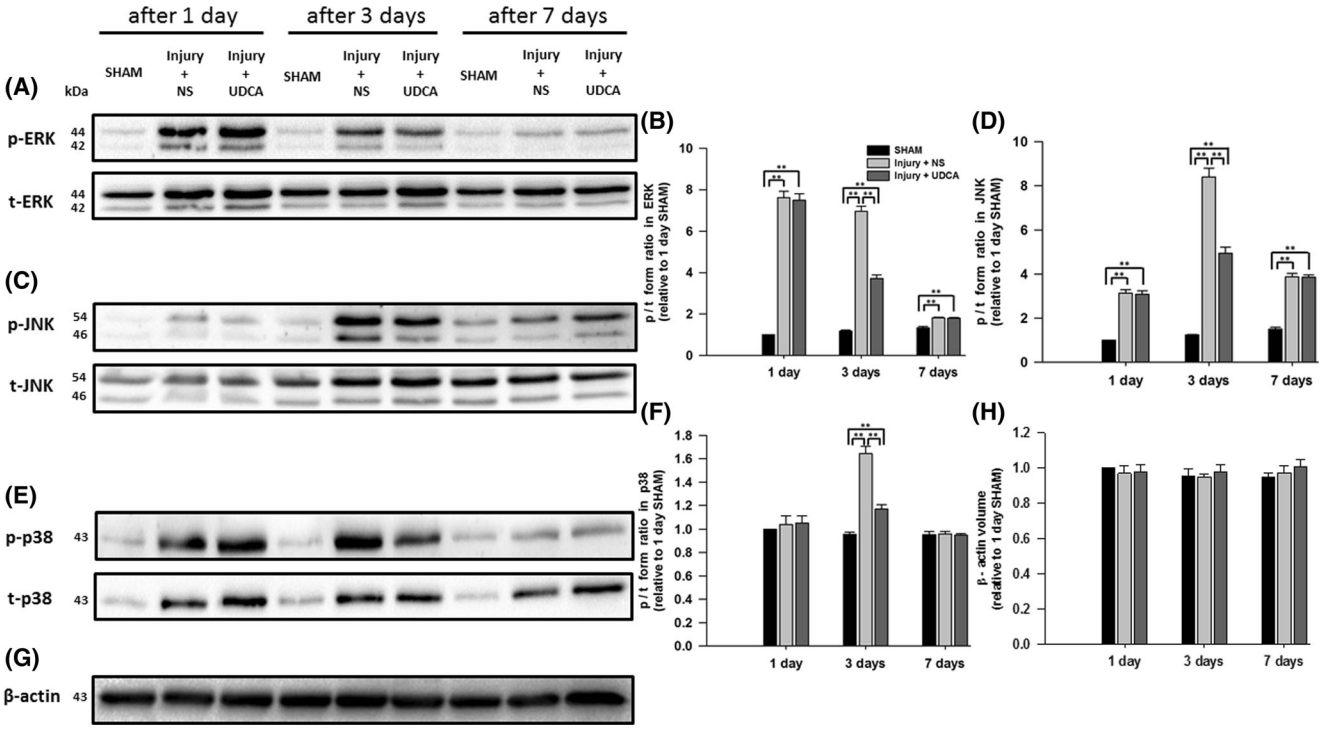

Fig. 8 Effect of UDCA on the phosphorylation of ERK, JNK, and p38 in injured spinal cord segments treated with UDCA (25 mg/kg/day, solubilized in 250 μL NS) or NS alone (250 μL) for 1, 3, and 7 days. Segments of the spinal cord (10 mm) including the lesion epicenter were collected on days 1, 3, or 7 after SCI. Immunoblotting was used to detect the phosphorylation forms or the total forms of ERK, JNK, and p38 in lysates prepared from the segments. β-actin was used as an internal control. The *p*/*t* form volume in the sham group on day 1 was set to onefold, and the ratio was relatively calculated and quantified. Representative images of the *p* and *t* forms of **a** ERK, **c** JNK, **e** p38, and **g** β-actin are shown. Quantitative analysis of the *p*/*t* forms of **b** ERK, **d** JNK, **f** p38, and **h** β-actin are shown. Results are the mean ± SEM of triplicate experiments: $*p < 0.05$ and $**p < 0.01$; significant differences among the three groups were demonstrated

SCI induces an acute activation of microglia followed by a delayed activation of astrocytes [27]. The activated astrocytes increase the production of GFAP, which results in multiple pro-inflammatory cytokines after SCI [28, 29]. We demonstrated that the expression of GFAP was significantly suppressed in the ROI using IF staining and quantification methods (Fig. 4 and Fig. S1a).

IL-10 has been reported to suppress the production of TNF and thereby exert an inhibitory influence on the activation of monocytes and other immune cells after SCI [26]. We verified that UDCA significantly increased IL-10 as compared to those in the injury + NS group on days 1, 3, and 7 after injury (Figs. 6d and 7d).

The phosphorylation of ERK, JNK, and the p38 signals in the MAPK pathway is a principle process during the inflammatory response after SCI [30]. On day 3 after the injury, the increased phosphorylation levels of ERK, JNK, and p38 in the injury + NS group were significantly inhibited by the UDCA treatment (Fig. 8b, d, f). However, the phosphorylation of the MAPK signals was not significantly inhibited in the injury + UDCA group on day 1 (Fig. 8b, d, f). UDCA did not inhibit the phosphorylation of the MAPK signals in 7 days as well (Fig. 8b, d, f). These phenomena are difficult to explain; however, when we consider that the pro-inflammatory cytokines were significantly decreased in the injury + UDCA group on day 7 (Figs. S1, 6a–c, and 7a–c), the inhibited phosphorylation in the MAPK signals on day 3 could have affected the reduction of the cytokines. Further studies are warranted to elucidate the exact mechanisms of the decreased cytokines.

In our current study, rats administrated UDCA showed no abnormal behaviors, such as hyper-locomotion and head-weaving behaviors [31] for 7 days. Cheng et al. demonstrated that 300 mg/kg/day of UDCA did not significantly affect body weight gain or daily food intake levels in rats for 10 days [32]. To the best of our knowledge, this is the first report to investigate the effects of UDCA in SCI rats.

Conclusion

Our study suggests that UDCA is a valuable anti-inflammatory agent and that it may serve as a therapeutic drug in SCI.

Funding Information This work was supported by Basic Science Research Program through the National Research Foundation of Korea (NRF) funded by the Ministry of Science, ICT, and future Planning (NRF-2016M3A9E8941668).

Compliance with Ethical Standards

Conflict of Interest The authors declare that they have no conflict of interest.

References

1. Thuret S, Moon LD, Gage FH (2006) Therapeutic interventions after spinal cord injury. Nat Rev Neurosci 7(8):628–643
2. Xu J, Kim GM, Ahmed SH, Xu J, Yan P, Xu XM, Hsu CY (2001) Glucocorticoid receptor-mediated suppression of activator protein-1 activation and matrix metalloproteinase expression after spinal cord injury. J Neurosci 21(1):92–97
3. Noble LJ, Donovan F, Igarashi T, Goussev S, Werb Z (2002) Matrix metalloproteinases limit functional recovery after spinal cord injury by modulation of early vascular events. J Neurosci 22(17):7526–7535
4. Hausmann ON (2003) Post-traumatic inflammation following spinal cord injury. Spinal Cord 41(7):369–378
5. Qiao F, Atkinson C, Kindy MS, Shunmugavel A, Morgan BP, Song H, Tomlinson S (2010) The alternative and terminal pathways of complement mediate post-traumatic spinal cord inflammation and injury. Am J Pathol 177(6):3061–3070
6. Beck KD, Nguyen HX, Galvan MD, Salazar DL, Woodruff TM, Anderson AJ (2010) Quantitative analysis of cellular inflammation after traumatic spinal cord injury: evidence for a multiphasic inflammatory response in the acute to chronic environment. Brain 133(Pt 2):433–447
7. Beattie MS (2004) Inflammation and apoptosis: linked therapeutic targets in spinal cord injury. Trends Mol Med 10(12):580–583
8. Bartholdi D, Schwab ME (1995) Methylprednisolone inhibits early inflammatory processes but not ischemic cell death after experimental spinal cord lesion in the rat. Brain Res 672(1–2):177–186
9. Gerndt SJ, Rodriguez JL, Pawlik JW, Taheri PA, Wahl WL, Micheals AJ, Papadopoulos SM (1997) Consequences of high-dose steroid therapy for acute spinal cord injury. J Trauma 42(2):279–284
10. Qian T, Guo X, Levi AD, Vanni S, Shebert RT, Sipski ML (2005) High-dose methylprednisolone may cause myopathy in acute spinal cord injury patients. Spinal Cord 43(4):199–203
11. Shi KQ, Fan YC, Liu WY, Li LF, Chen YP, Zheng MH (2012) Traditional Chinese medicines benefit to nonalcoholic fatty liver disease: a systematic review and meta-analysis. Mol Biol Rep 39(10):9715–9722
12. Bachrach WH, Hofmann AF (1982) Ursodeoxycholic acid in the treatment of cholesterol cholelithiasis. part I. Dig Dis Sci 27(8):737–761
13. Beuers U, Boyer JL, Paumgartner G (1998) Ursodeoxycholic acid in cholestasis: potential mechanisms of action and therapeutic applications. Hepatology 28(6):1449–1453
14. Cirillo NW, Zwas FR (1994) Ursodeoxycholic acid in the treatment of chronic liver disease. Am J Gastroenterol 89(9):1447–1452
15. Lazaridis KN, Gores GJ, Lindor KD (2001) Ursodeoxycholic acid mechanisms of action and clinical use in hepatobiliary disorders. J Hepatol 35(1):134–146
16. Ko WK, Lee SH, Kim SJ, Jo MJ, Kumar H, Han IB, Sohn S (2017) Anti-inflammatory effects of ursodeoxycholic acid by lipopolysaccharide-stimulated inflammatory responses in RAW 264.7 macrophages. PLoS One 12(6):e0180673
17. Fleming JC, Norenberg MD, Ramsay DA, Dekaban GA, Marcillo AE, Saenz AD, Pasquale-Styles M, Dietrich WD et al (2006) The cellular inflammatory response in human spinal cords after injury. Brain 129(Pt 12):3249–3269
18. Donnelly DJ, Popovich PG (2008) Inflammation and its role in neuroprotection, axonal regeneration and functional recovery after spinal cord injury. Exp Neurol 209(2):378–388
19. Ropper AE, Zeng X, Anderson JE, Yu D, Han I, Haragopal H, Teng YD (2015) An efficient device to experimentally model compression injury of mammalian spinal cord. Exp Neurol 271:515–523
20. Basso DM, Beattie MS, Bresnahan JC (1995) A sensitive and reliable locomotor rating scale for open field testing in rats. J Neurotrauma 12(1):1–21
21. Kumar H, Jo MJ, Choi H, Muttigi MS, Shon S, Kim BJ, Lee SH, Han IB (2017) Matrix Metalloproteinase-8 inhibition prevents disruption of blood-spinal cord barrier and attenuates inflammation in rat model of spinal cord injury. Mol Neurobiol 54:3578–3590
22. Collins TJ (2007) ImageJ for microscopy. BioTechniques 43(1 Suppl):25–30
23. Schmittgen TD, Livak KJ (2008) Analyzing real-time PCR data by the comparative C(T) method. Nat Protoc 3(6):1101–1108
24. Hayashi M, Ueyama T, Nemoto K, Tamaki T, Senba E (2000) Sequential mRNA expression for immediate early genes, cytokines, and neurotrophins in spinal cord injury. J Neurotrauma 17(3):203–218
25. Saiwai H, Kumamaru H, Ohkawa Y, Kubota K, Kobayakawa K, Yamada H, Yokomizo T, Iwamoto Y et al (2013) Ly6C+ Ly6G- myeloid-derived suppressor cells play a critical role in the resolution of acute inflammation and the subsequent tissue repair process after spinal cord injury. J Neurochem 125(1):74–88
26. Bethea JR, Nagashima H, Acosta MC, Briceno C, Gomez F, Marcillo AE, Loor K, Green J et al (1999) Systemically administered interleukin-10 reduces tumor necrosis factor-alpha production and significantly improves functional recovery following traumatic spinal cord injury in rats. J Neurotrauma 16(10):851–863
27. Sweitzer SM, Colburn RW, Rutkowski M, DeLeo JA (1999) Acute peripheral inflammation induces moderate glial activation and spinal IL-1beta expression that correlates with pain behavior in the rat. Brain Res 829(1–2):209–221
28. Yin X, Yin Y, Cao FL, Chen YF, Peng Y, Hou WG, Sun SK, Luo ZJ (2012) Tanshinone IIA attenuates the inflammatory response and apoptosis after traumatic injury of the spinal cord in adult rats. PLoS One 7(6):e38381
29. Bareyre FM, Schwab ME (2003) Inflammation, degeneration and regeneration in the injured spinal cord: Insights from DNA microarrays. Trends Neurosci 26(10):555–563
30. Genovese T, Esposito E, Mazzon E, Muia C, Di Paola R, Meli R, Bramanti P, Cuzzocrea S (2008) Evidence for the role of mitogen-activated protein kinase signaling pathways in the development of spinal cord injury. J Pharmacol Exp Ther 325(1):100–114
31. Hiyoshi T, Kambe D, Karasawa J, Chaki S (2014) Differential effects of NMDA receptor antagonists at lower and higher doses on basal gamma band oscillation power in rat cortical electroencephalograms. Neuropharmacology 85:384–396
32. Cheng Y, Tauschel HD, Nilsson A, Duan RD (1999) Ursodeoxycholic acid increases the activities of alkaline sphingomyelinase and caspase-3 in the rat colon. Scand J Gastroenterol 34(9):915–920